Aquaculture 599 (2025) 742139

Contents lists available at ScienceDirect

Aquaculture

journal homepage: www.elsevier.com/locate/aquaculture

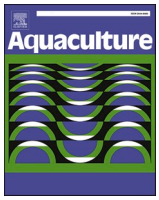

Dynamics of proximate composition, fatty acid profile and transcriptome response to low-temperature stress in muscle tissues of spotted sea bass (*Lateolabrax maculatus*)

Cong Liu [a,1], Yuan Zheng [a,1], Haishen Wen [a], Chong Zhang [a], Yonghang Zhang [a], Lingyu Wang [a], Donglei Sun [a], Kaiqiang Zhang [a], Xin Qi [a], Yun Xia [b,**], Yun Li [a,*]

[a] *Key Laboratory of Mariculture, Ministry of Education (KLMME), Ocean University of China, Qingdao 266003, China*
[b] *National Fisheries Technology Extension Center, Beijing 100125, China*

ARTICLE INFO

Keywords:
Cold stress
Nutritional composition
Transcriptomic analysis
Lateolabrax maculatus

ABSTRACT

Spotted sea bass (*Lateolabrax maculatus*) is widely farmed as an economical fish species in China's coastal regions. However, limited information is available on the molecular mechanisms underlying the low-temperatures response for this species. In the present research, we investigated the dynamic changes in the proximate composition and fatty acid profile of muscle tissue after 0, 24, 48, and 72 h of low-temperature stress using 90 experimental fish individuals, with particular emphasis on the underlying molecular mechanisms in response to low-temperature stress. Our results revealed a significant ($p < 0.05$) decrease in crude fat and protein content, while a notable increase in moisture with prolonged exposure to low temperature. Additionally, the fatty acid composition exhibited a marked decrease in saturated fatty acids and an increase in monounsaturated fatty acids and polyunsaturated fatty acids. Transcriptomic sequencing of muscle tissue under low temperature identified 3337 differentially expressed genes (DEGs), which were categorized into six clusters. Hub genes were identified by protein-protein interactions networks, including *pik3ca*, *actn1* and *mapk14b* in cluster 3, *psma3*, *ubqln4* and *hspa5* in cluster 4, *stat3*, *mapk8b* and *cdk2* in cluster 5, as well as *hsp90aa1.1*, *ptk* and *actc1a* in cluster 6. The KEGG pathway enrichment analysis for the four regular-expressed clusters showed significant ($p < 0.05$) enrichment in glutathione metabolism, apoptosis, adipocytokine signaling pathways and phagosomes in two significantly ($p < 0.05$) up-regulated clusters (cluster4 and 5), while down-regulated clusters (clusters 3 and 6) were enriched for pathways related to actin cytoskeleton, focal adhesion and ECM-receptor interaction. Furthermore, 571 differential alternative splicing (DAS) events were identified, and KEGG pathway enrichment of genes overlapping between DEGs and DAS genes revealed a significant ($p < 0.05$) association with glutathione metabolism, insulin signaling pathway, glycolysis / gluconeogenesis, regulation of actin cytoskeleton, cysteine and methionine metabolism, ferroptosis, ErbB signaling pathway, FoxO signaling pathway and adipocytokine signaling pathway. In summary, ubiquitin mediated proteolysis and adipocytokine signaling emerged as key regulatory pathways for the observed changes in proteins and fatty acids compositions. This investigation contributes to the understanding of the impacts of low-temperatures on the spotted sea bass muscle tissue, providing novel perspectives for understanding the molecular mechanisms of fish responses to cold stress.

1. Introduction

As a widely cultured economic fish in China's coastal areas, spotted sea bass (*Lateolabrax maculatus*) has a vast market potential and enormous economic value (Liu et al., 2023). According to the statistics of the Fisheries Yearbook (China, 2023), the average annual production of this species exceeds 200,000 tons and continues to grow year by year (Ren et al., 2022). Ensuring a steady supply of high-quality seedlings is crucial to meeting the industry's increasing demand. Population genetics and mitochondrial genome analyses divide the spotted sea bass population

* Correspondence to: Y. Li, Ocean University of China, No. 5 Yushan road, Qingdao 266003, China.
** Correspondence to: Y. Xia, National Fisheries Technology Extension Center, No. 18 Maizidian street, Chaoyang District, Beijing 100125, China.
E-mail addresses: xiayunnftec@sina.com (Y. Xia), yunli0116@ouc.edu.cn (Y. Li).
[1] The two authors contribute equally to this work.

https://doi.org/10.1016/j.aquaculture.2025.742139
Received 21 September 2024; Received in revised form 10 December 2024; Accepted 8 January 2025
Available online 9 January 2025

into two major groups: the Bohai Gulf and Beibu Gulf populations, representing northern and southern wild populations, respectively (Chen et al., 2023a, 2023b; Gong et al., 2020). The Bohai Gulf population is favored by farmers for its robustness, resilience and earlier natural spawning compared to the southern population (Zhao et al., 2018). However, extreme cold weather during winter increases farming costs, exposes this species to environmental stress and mortality risks. Therefore, how to promote the ability of low-temperature tolerance has emerged as an urgent issue in the development of sustainable aquaculture in spotted sea bass.

Muscle, the largest tissue in fish, comprises approximately 40–50 % of body weight (Bai et al., 2022), and is particularly vulnerable to low-temperature stress (Dietrich et al., 2018). Structural changes and damage in muscle tissue morphology under low-temperature conditions have been well-documented. For example, paraffin sections showed severe histopathological damage in the muscle tissue of silver pomfret (*Pampus argenteus*) at 8 °C (Zhang et al., 2022). Additionally, muscle is an essential location for lipid metabolism and particularly acts as a key player in the synthesis and degradation of fatty acids. At low temperatures, significant ($p < 0.05$) changes in protein content were observed in green sunfish cells (Ibarz et al., 2005; Shaklee et al., 1977). A well-known response to lower ambient temperatures is homeoviscous adaptation, characterized by increased unsaturation of fatty acids to maintain membrane fluidity and permeability (Biederman et al., 2021). The important role of lipid metabolism in coping with low-temperature stress has also been reported in various fish species, including striped bass (*Morone saxatilis*) (Araújo et al., 2021), juvenile European seabass (*Dicentrarchus labrax*) (Zhang et al., 2021) and a cave fish (*Onychostoma macrolepis*) (Deng et al., 2020). Furthermore, the relative expression levels of peroxisome proliferator-activated receptor alpha (*PPAR-α*) and *PPAR-γ* that regulate lipid metabolism were up-regulated under low temperatures in spotted sea bass liver (Wang et al., 2022). However, the molecular mechanisms underpinning the cold-temperature response are poorly understood in spotted sea bass.

High-throughput transcriptomic sequencing technology offers a powerful tool to determine differences in gene expression in fish under low temperatures. For instance, transcriptome sequencing of liver tissue in black porgy (*Acanthopagrus schlegelii*) identified numerous differentially expressed genes (DEGs), and with enrichment results indicating that metabolism, signal transduction and apoptosis were affected by acute cold stress (Wang et al., 2023). In small yellow croaker (*Larimichthys polyactis*), transcriptome sequencing of cold-resistant and cold-sensitive individuals exposed to 4 °C revealed various mechanisms that reduce cold shock damage, including regulation of autophagy, glycerolipid metabolism, ECM receptor interaction and focal adhesion pathways (Liu et al., 2020a, 2020b). Differential alternative splicing (DAS), a common molecular mechanism of post-transcriptional regulation, was identified after cold stress in zebrafish (*Danio rerio*) and Atlantic killifish (*Fundulus heteroclitus*) (Healy and Schulte, 2019). Functional enrichment of DAS genes showed that muscle contraction was involved in cold adaptation (Healy and Schulte, 2019). In common carp (*Cyprinus carpio*), an alternatively spliced isoforms of Δ9-acyl CoA desaturase was observed to be up-regulated expression in cold acclimation (Polley et al., 2003). Therefore, digging into transcriptomic data using bioinformatic approach to identify DAS genes will assist in elucidating the mechanisms of post-transcriptional regulation under low-temperature stress.

The aims of this study were to explore the dynamic changes in proximate composition and fatty acid profile in spotted sea bass muscle tissue under low temperature and to elucidate the molecular mechanisms responsible for low-temperature stress using transcriptomic analysis. The conclusions of this research could deepen our knowledge of how spotted sea bass adapt to cold challenges and assist aquaculture managers in applying alternative strategies to improve cold tolerant abilities and reduce winter mortality.

2. Materials and methods

2.1. Ethics statement

In this research, experimental sample collection followed the Guidelines for the Care and Use of Laboratory Animals in China and were approved by the Animal Research and Ethics Committees of Ocean University of China (Permit Number: 20141201).

2.2. Experimental design and sampling

To understand the impacts of low temperatures on the spotted sea bass muscle tissue, we randomly selected 90 healthy fish individuals (body length: 22.70 ± 1.34 cm, body weight: 103.97 ± 3.85 g) for low-temperature stress experiments. The experimental fish were divided into three parallel replicate nets with a density of 30 fish in each replicate and domesticated for two weeks at Shuangying Aquatic Seeding Co., Ltd., located at Dongying city, Shandong province, under the following conditions: temperature of 15 ± 1 °C, salinity of 25.67 ± 0.47, pH value of 8.38 ± 0.12, dissolved oxygen content more than 7.0 mg/L. During the period of domestication, we fed the fish with commercial feed (Zhuhai Haiwei Feed Co., Ltd., China) and started the experiment 24 h after stopping feeding. When the experiment started, the temperature decreased uniformly at an average rate of 1 °C/h from 15 °C to 5 °C for low-temperature stress. The experimental period was designed to be 72 h to detect the dynamic response of the spotted sea bass to low-temperature stress. To minimize experimental error, three individuals were randomly selected from each replicate net for every experimental group, meaning each experimental group had a total of nine individuals sampled (Three replicates × three individuals). After anesthetized with MS-222 bath (100 mg/L) (Sun et al., 2019) within two minutes, a 2 cm^3 volume of skeletal muscle located below the first dorsal fin was quickly excised using a surgical scalpel, excluding the scales and skin. The skeletal muscle tissue sampled at domestication temperatures (15 °C) as control group, and at 0 h, 6 h, 12 h, 24 h, 48 h and 72 h following exposure to low-temperature stress as experimental groups, labeled as control group, 0 h group, 6 h group, 12 h group, 24 h group, 48 h group and 72 h group, respectively. The muscle samples were divided into two portions, one was placed at −40 °C for determination of proximate composition and fatty acid content, and the other muscle tissue was snap frozen with liquid nitrogen for RNA extraction.

2.3. Measurement of proximate composition and fatty acid profile

The proximate composition of muscle consists of moisture, crude protein, crude fat and ash (Ahmed et al., 2022). Muscle tissue was freeze-dried using ALPHA1–2 (Christ, Germany), and then pulverized and stored in a desiccator. Moisture was calculated by freeze-drying to constant weight and calculating the weight difference. The crude fat was measured based on the Soxhlet extraction method using the Soxhlet Extraction System B-811 (Buchi, Switzerland). The determination of crude protein was carried out using an instrument Kjeltec 8400 Analyzer Unit (Foss, Denmark) based on the method of Kjeldahl method. The ash content was determined by burning the dried samples in a muffle furnace at 550 °C until constant weight and the difference in weight was calculated.

For the measurement of muscle fatty acid profile, the samples were processed following the HCL-methanol method (Zuo et al., 2012). Briefly, approximately 100 mg of freeze-dried sample was placed into a 20 mL volumetric spiral glass tube with a plastic cap. Then, 3 mL of 1 mol/L of potassium hydroxide-methanol solution was added and the mixture was heated in a 72 °C water bath for 20 min. After cooling to room temperature, 3 mL of 2 mol/L hydrochloric acid-methanol solution was added, and the mixture was heated for 20 min at a 72 °C water bath. Finally, 1 mL of hexane was added and the solution was mixed thoroughly to make the solution phased. The solution separating the upper

layers was used to measure fatty acid composition using HP5890 II gas chromatograph (Agilent Technologies, USA).

2.4. RNA extraction and sequencing

After isolation of total RNA using SparkZol reagent (SparkJade, China), the concentration, OD_{260}/OD_{280} value and quality were assessed using Biodropsis BD-1000 (Beijing, China). Total RNA of three fish within the same parallel replicate nets at each sampling time point was mixed and three biological replicates were set up for sequencing to eliminate individual differences. Subsequently, the mixed high-quality RNA was transported with dry ice at low temperatures to Novogene (Beijing, China). The mRNA was fragmented into small pieces and then reverse-transcribed into cDNA. Short adapter sequences were ligated to both ends of the cDNA fragments to amplify using PCR to generate sufficient material for sequencing. The PCR conditions were as follows: an initial denaturation at 95 °C for 5 min, followed by 40 cycles of 95 °C for 15 s (denaturation), 60 °C for 30 s (annealing), and 72 °C for 1 min (extension). A final extension step was carried out at 72 °C for 5 min to ensure complete extension of the products. After that, a total of 12 sequencing libraries were constructed using the NEB Next UltraTM RNA Library Prep Kit for Illumina according to the flow of the manufacturer's instructions, including control group, 6 h group, 12 h group and 24 h group. The libraries were sequenced on the Illumina NovaSeq 6000 platform to yield 150 bp paired-end reads.

2.5. Data filtering and differential expression analysis

Quality assessment was performed using FastQC (https://github.com/s-andrews/FastQC). After that, the raw data was treated with Trimmomatic (Bolger et al., 2014) to remove low-quality reads and adapter to generate clean reads. Subsequently, clean reads were mapped to the spotted sea bass genome sequence (PRJNA408177) using Hisat2 (Kim et al., 2019). The raw count matrices were generated using Subread (Liao et al., 2014), and then calculated to FPKM, which represents gene expression level. Differential expression analysis was performed with the raw count matrices using DESeq2 (Love et al., 2014), significant threshold was adjusted p-value <0.05 and $|\log_2(\text{FoldChange})| > 1$.

2.6. Time-series expression analysis and hub gene identification

To explore gene expression patterns with time series, we performed soft clustering analysis of the gene expression patterns (FPKM values) of the time-series data using the R package of Mfuzz (v 2.48.0) (Kumar and Futschik, 2007) with a fuzzy c-means algorithm, and the main parameter was set to centers = 6.

To identify the hub genes within the cluster from the time-series expression analysis, the DEGs were aligned to the String (https://cn.string-db.org/) for construction of protein-protein interactions (PPIs) networks with default thresholds. The identification of hub genes was carried out using the cytoHubba plugin from Cytoscape (Shannon et al., 2003) through the MCC analysis algorithm.

2.7. Alternative splicing analysis

To identify DAS events responding to low-temperature stress in spotted sea bass, rMATS was run to identify DAS (Shen et al., 2014), which is an efficient bioinformatic tool for alternative splicing analysis using RNA-seq data. The p-value was determined using the likelihood-ratio test, and IncLevel was corrected for p-value by the Benjamini Hochberg algorithm to obtain the FDR value. A threshold of FDR < 0.05 was used for identifying DAS events.

2.8. Pathway enrichment analysis

To explore the pathways in DAS genes and DEGs, pathway enrichment analysis was conducted at the KOBAS online platform (Bu et al., 2021). Significant enrichment p-values were corrected by Benjamini-Hochberg method with a threshold of <0.05. The enrichment results were visualized with ggplot2 package (Wickham, 2011).

2.9. Validation of RNA-seq data

To verify the results of transcriptomic analysis, nine DEGs were randomly selected for qPCR validation from the control and 24 h groups. In detail, total RNA was isolated as previously described, and then cDNA was generated by reverse transcription with 500 ng/uL of RNA using the cDNA synthesis solution (Shanghai Yeasen Biotechnology Co., Ltd., China). The specific primers of validated genes were designed by Primer 5.0 (Table 1), and *18 s* as the reference gene. The relative expression levels were detected by StepOnePlus Real-Time PCR system (ABI, USA).

2.10. Statistical analysis

Statistical analysis was performed using the SPSS software (v 26.0). All results are presented as mean ± standard deviation. The differences in muscle fatty acid profile between the control and treatment groups at each time point were compared by one-way ANOVA followed by Tukey's post hoc test, with $p < 0.05$ as the significant threshold.

3. Results

3.1. Changes in muscle proximate composition

As illustrated in Fig. 1, changes in muscle proximate composition of spotted sea bass during low-temperature stress indicated that moisture, crude fat and crude protein were significantly ($p < 0.05$) affected under cold. In detail, the moisture increased significantly ($p < 0.05$) with the prolongation of the stress time, and the contents reached the maximum value at 48 h, which was not significantly ($p < 0.05$) different from that at 72 h. The crude fat and crude protein contents decreased gradually over time with the duration of low-temperature stress. However, no significant ($p < 0.05$) difference was observed between the 48 h and 72 h groups for any of the parameters, suggesting that the effects of low-temperature stress may plateau after 48 h. The ash contents showed no significant ($p < 0.05$) change throughout the low-temperature stress process.

Table 1
Primers for qPCR validation.

Gene	Sequence of primers (5′ to 3′)
Heat shock protein family A member 5 (*hspa5*)	F: TGACACCTGAGGATATTGAGCG R: TCCACTGCCTTCTCAATGGT
Proteasome 26S subunit, ATPase 3 (*psmc3*)	F: TCCCGCAAGATGAACGTCAG R: TTCATGGTTCAGCTCCGTGG
Thioredoxin like 1 (*txnl1*)	F: TGTCGGAGGAAGACTGCAAAGATG R: TCACTCATGTTGGTGGCCTGT
Signal transducer and activator of transcription 3 (*stat3*)	F: TCAAGACATCAGGAAGCGGG R: CTGGGACAACTCTCCTTGGC
FKBP prolyl isomerase 5 (*fkbp5*)	F: GGAGTGTGGCACTGGGATAG R: TAGCCGCAAGAAACACATCG
Myogenic differentiation 1 (*myod1*)	F: AAGGCGACGGCTCAGTAAAG R: ATCCATCATGCCATCGGAGC
Nuclear receptor corepressor 1 (*ncor1*)	F: GTGCCATCAACAACACACCC R: ATTTCCGGCTGTTGGCTTTG
PNN interacting serine and arginine rich protein (*pnisr*)	F: GCCAAATCTAGCAGGAGACAC R: CCTTGAGCGACTACGTTTGG
Pinin, desmosome associated protein (*pnn*)	F: ACAAGCACCAAACACCAGTC R: CGAGGCCAGGGATGATGAAAT
18S ribosomal RNA (*18 s*)	F: GGGTCCGAAGCGTTTACT R: TCACCTCTAGCGGCACAA

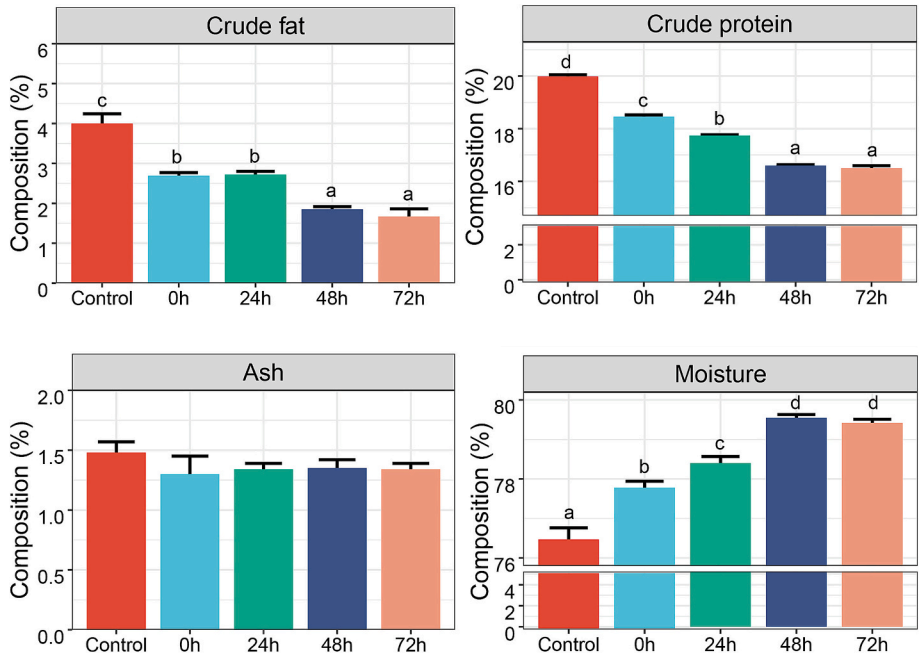

Fig. 1. Dynamics of proximate component after low-temperature stress in spotted sea bass muscle tissue.

Table 2
Changes of muscle fatty acid profile of spotted sea bass muscle under low-temperature stress.

Fatty acid		Content(%)				
		Control	0 h	24 h	48 h	72 h
SFA	C4:0 (Butryic acid)	0.25 ± 0.02	0.20 ± 0.01	0.21 ± 0.01	0.22 ± 0.01	0.23 ± 0.01
	C6:0 (Caproic acid)	0.43 ± 0.02^{b}	0.27 ± 0.02^{a}	0.27 ± 0.01^{a}	0.27 ± 0.01^{a}	0.28 ± 0.01^{a}
	C8:0 (Caprylic acid)	0.17 ± 0.03^{ab}	0.15 ± 0.02^{a}	0.12 ± 0.02^{a}	0.12 ± 0.01^{a}	0.21 ± 0.01^{b}
	C10:0 (Capric acid)	0.21 ± 0.01	0.21 ± 0.01	0.22 ± 0.01	0.23 ± 0.01	0.23 ± 0.01
	C11:0 (Undecanoic acid)	0.13 ± 0.01	0.13 ± 0.01	0.13 ± 0.01	0.14 ± 0.01	0.14 ± 0.01
	C12:0 (Lauric acid)	0.26 ± 0.01^{b}	0.19 ± 0.01^{a}	0.20 ± 0.01^{a}	0.20 ± 0.01^{a}	0.20 ± 0.01^{a}
	C13:0 (Tridecanoic acid)	3.15 ± 0.05^{c}	1.80 ± 0.22^{b}	1.32 ± 0.04^{a}	1.37 ± 0.01^{a}	1.43 ± 0.02^{a}
	C14:0 (Myristic acid)	3.35 ± 0.14^{c}	2.94 ± 0.02^{b}	2.52 ± 0.04^{a}	2.39 ± 0.11^{a}	2.57 ± 0.04^{a}
	C15:0 (Pentadecanoic acid)	0.44 ± 0.04^{b}	0.21 ± 0.01^{a}	0.21 ± 0.01^{a}	0.21 ± 0.01^{a}	0.21 ± 0.01^{a}
	C16:0 (Palmitic acid)	16.78 ± 0.20^{b}	10.14 ± 0.66^{a}	9.57 ± 0.17^{a}	9.70 ± 0.10^{a}	9.37 ± 0.20^{a}
	C17:0 (Heptadecanoic acid)	0.45 ± 0.06	0.30 ± 0.02	0.34 ± 0.01	0.33 ± 0.01	0.37 ± 0.05
	C18:0 (Stearic acid)	2.21 ± 0.11^{b}	0.70 ± 0.14^{a}	0.56 ± 0.03^{a}	0.67 ± 0.03^{a}	0.65 ± 0.05^{a}
	C20:0 (Arachidic acid)	4.65 ± 0.08^{b}	2.48 ± 0.26^{a}	2.48 ± 0.17^{a}	2.51 ± 0.10^{a}	2.44 ± 0.06^{a}
	C21:0 (Henicosanoic acid)	0.64 ± 0.08	0.65 ± 0.03	0.71 ± 0.01	0.71 ± 0.01	0.67 ± 0.02
	C24:0 (Lignoceric acid)	1.39 ± 0.15^{c}	0.24 ± 0.01^{a}	0.44 ± 0.06^{ab}	0.54 ± 0.03^{b}	0.55 ± 0.04^{b}
	ΣSFA (Saturated fatty acid)	34.52 ± 0.38^{b}	20.61 ± 0.64^{a}	19.33 ± 0.25^{a}	19.60 ± 0.37^{a}	19.56 ± 0.12^{a}
MUFA	C14:1 (Myristoleic acid)	1.07 ± 0.08	1.17 ± 0.03	1.19 ± 0.03	1.20 ± 0.01	1.20 ± 0.01
	C15:1 (cis-10-Pentadecenoic acid)	2.35 ± 0.41	2.38 ± 0.09	2.46 ± 0.07	2.40 ± 0.10	2.48 ± 0.10
	C16:1 (Palmitoleic acid)	8.49 ± 0.12	8.52 ± 0.19	8.44 ± 0.10	8.62 ± 0.01	8.57 ± 0.21
	C17:1 (cis-10-Heptadecenoic acid)	1.05 ± 0.08^{a}	1.39 ± 0.01^{b}	1.63 ± 0.07^{c}	1.57 ± 0.03^{c}	1.61 ± 0.02^{c}
	C18:1 trans (tran-Octadecenoic acid)	13.41 ± 0.25^{a}	15.54 ± 0.23^{b}	15.61 ± 0.17^{b}	15.14 ± 0.20^{b}	15.06 ± 0.08^{b}
	C18:1 cis (cis-Octadecenoic acid)	2.15 ± 0.13^{a}	2.60 ± 0.06^{b}	2.50 ± 0.08^{b}	2.65 ± 0.02^{b}	2.59 ± 0.07^{b}
	C20:1 n9 (9-Eicosenoic acid)	0.99 ± 0.02	1.04 ± 0.03	1.02 ± 0.09	1.00 ± 0.01	1.11 ± 0.06
	ΣMUFA (Monounsaturated fatty acid)	29.51 ± 0.26^{a}	32.65 ± 0.43^{b}	32.86 ± 0.31^{b}	32.59 ± 0.15^{b}	32.61 ± 0.17^{b}
n-3 PUFA	C18:3 n-3 (α-Linolenic acid, ALA)	1.20 ± 0.01^{a}	1.40 ± 0.06^{b}	1.48 ± 0.01^{bc}	1.53 ± 0.02^{c}	1.54 ± 0.04^{c}
	C20:5 n-3 (Eicosapentaenoic Acid, EPA)	7.30 ± 0.08^{a}	10.33 ± 0.77^{b}	11.04 ± 0.03^{bc}	11.84 ± 0.31^{c}	11.13 ± 0.11^{bc}
	C22:6 n-3 (Docosahexaenoic acid, DHA)	18.11 ± 0.51^{a}	21.35 ± 0.38^{b}	22.03 ± 0.35^{b}	21.06 ± 0.33^{b}	21.82 ± 0.33^{b}
	∑n-3 (n-3 PUFAs)	26.60 ± 0.48^{a}	33.08 ± 1.18^{b}	34.55 ± 0.31^{b}	34.44 ± 0.53^{b}	34.48 ± 0.19^{b}
n-6 PUFA	C18:2 trans (trans-Linoleic acid)	0.47 ± 0.28^{a}	2.56 ± 0.05^{b}	2.66 ± 0.12^{b}	2.65 ± 0.05^{b}	2.49 ± 0.18^{b}
	C18:2 cis (cis-Linoleic acid)	7.35 ± 0.05^{a}	9.55 ± 0.05^{b}	9.05 ± 0.05^{b}	9.18 ± 0.05^{b}	9.32 ± 0.32^{b}
	C20:4 n-6 (Arachidonic acid, ARA)	1.55 ± 0.02	1.55 ± 0.02	1.56 ± 0.01	1.54 ± 0.01	1.55 ± 0.01
	∑n-6 (n-6 PUFAs)	9.37 ± 0.33^{a}	13.66 ± 0.11^{b}	13.27 ± 0.08^{b}	13.37 ± 0.09^{b}	13.35 ± 0.23^{b}
	ΣPUFA (Polyunsaturated fatty acid)	65.48 ± 0.38^{a}	79.40 ± 0.64^{b}	80.68 ± 0.25^{b}	80.40 ± 0.37^{b}	80.45 ± 0.12^{b}
	∑n-6/∑n-3	0.35 ± 0.02	0.41 ± 0.02	0.38 ± 0.01	0.39 ± 0.01	0.39 ± 0.01
	DHA/EPA	2.48 ± 0.09^{c}	2.09 ± 0.13^{b}	2.00 ± 0.04^{ab}	1.78 ± 0.04^{a}	1.96 ± 0.05^{ab}
	ΣPUFA/ΣSFA	1.90 ± 0.03^{a}	3.86 ± 0.15^{b}	4.18 ± 0.07^{c}	4.10 ± 0.10^{bc}	4.11 ± 0.03^{bc}

Note: The statistical analysis is performed by one-way ANOVA followed by Tukey's post hoc test. The number of samples in each group is nine. Different superscript letters indicate significant differences ($p < 0.05$).

3.2. Changes in muscle fatty acid profile

We detected 28 fatty acid compositions in the muscle of spotted sea bass, including 15 saturated FAs (SFAs), 6 polyunsaturated FAs (PUFAs) and 7 monounsaturated FAs (MUFAs) (Table 2). Most of the SFA content decreased significantly ($p < 0.05$) during the low-temperature stress, including C6:0, C8:0, C12:0, C13:0, C14:0, C15:0, C16:0, C18:0, C20:0 and C24:0, while C4:0, C10:0, C11:0, C17:0 and C21:0 showed no significant ($p < 0.05$) changes. For the MUFA, three MUFAs exhibited significant ($p < 0.05$) increases in content, including C17:1, C18:1 cis and C18:1 trans, and the remaining MUFAs showed no significant ($p < 0.05$) changes in content. Among the PUFAs, both n-3 and n-6 PUFAs showed a significant ($p < 0.05$) increase during low-temperature stress, except for C20:4 n-6 (ARA) in n-6 PUFAs. In addition, the values of DHA/EPA and ΣPUFA/ΣSFA showed significant ($p < 0.05$) changes. Overall, SFAs, MUFAs and PUFAs were significantly ($p < 0.05$) affected after low-temperature stress.

3.3. Overview of RNA-seq data

Transcriptome sequencing was performed on the spotted sea bass muscle tissues from this low-temperature stress experiment, and the statistical results demonstrated that 79.36 Gb of raw bases were generated. After quality control, 77.53 Gb of clean bases were used for subsequent analyses, with an average 6.58 Gb clean bases per sample. For sequencing quality assessment, the Q20 value ranged from 96.56 to 97.04 %, with an average of 96.83 %, Q30 value ranged from 91.06 to 92.25 %, with an average 91.82 %, and GC content ranged from 49.27 to 50.70 %, with an average content of 50.07 %. After aligning to the reference genome sequence, the alignment rate ranged from 91.89 to 95.31 %, with an average alignment rate of about 93.51 %, showing a high quality of sequencing data, and can be used for subsequent analysis.

3.4. Identification of differentially expressed genes

Differential expression analysis was undertaken at 6 h, 12 h and 24 h with the control group, respectively. After that, 3337 DEGs were identified among the three comparison groups. Specifically, 2163 DEGs were identified in the 6h_vs_Control group, including 1190 up-regulated and 973 down-regulated DEGs (Fig. 2A). In the 12h_vs_Control group, 2033 DEGs were identified, with 941 up-regulated and 1192 down-regulated DEGs (Fig. 2B). While in the 24 h_vs_Control group, 2416 DEGs were

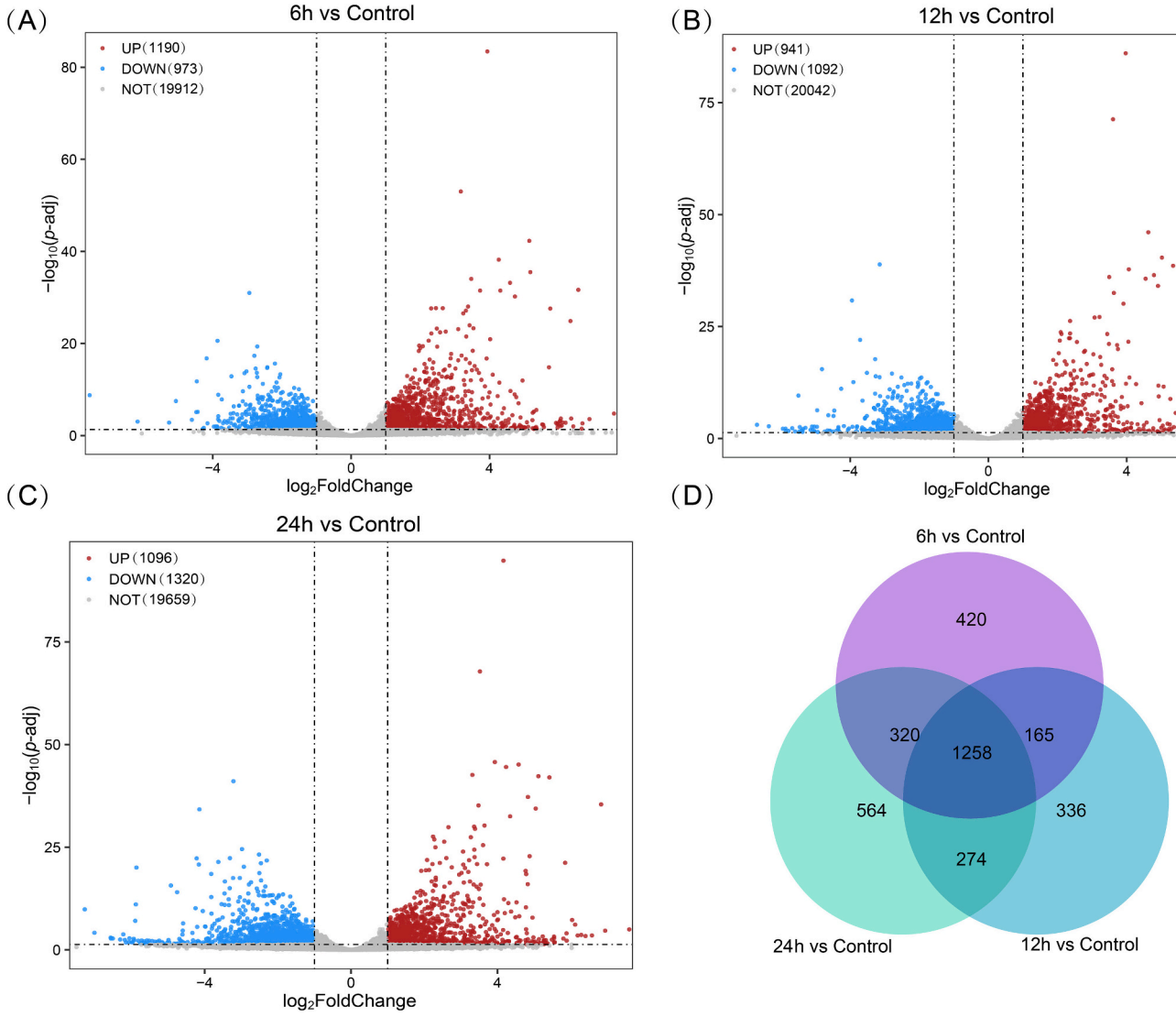

Fig. 2. Identification of differentially expressed genes (DEGs) in the 6 h vs Control (A), 12 h vs Control (B) and 24 h vs Control (C). Red dots represent up-regulated DEGs, blue dots represent down-regulated DEGs and grey dots represent DEGs that are not differentially expressed. (D) Venn diagram of DEGs among the three comparison groups. (For interpretation of the references to colour in this figure legend, the reader is referred to the web version of this article.)

identified, including 1096 up-regulated and 1320 down-regulated DEGs (Fig. 2C). In addition, 1258 DEGs overlapped in all comparison groups (Fig. 2D).

3.5. Temporal expression analysis and hub gene identification

Based on the time-dependent trends of DEG expression levels under low-temperature stress, we divided DEGs into six clusters, containing 496, 613, 451, 608, 445 and 724 DEGs, respectively (Fig. 3A). Among these six clusters, cluster 1 and cluster 2 displayed an irregular gene expression pattern, with the showing an increasing trend and then decreasing expression, while in cluster 2, it decreased and then increased. Notably, the expression levels of DEGs in clusters 3 and 6 maintained a constant decreasing trend throughout the stress, while DEGs in clusters 4 and 5 were significantly ($p < 0.05$) increased.

To identify the hub genes with regular variations in gene expression patterns, four cluster (cluster 3, 4, 5 and 6) were used to construct PPI networks, respectively. In cluster 3, ten DEGs were identified as hub genes, including *syk*, *ptpn11b*, *pxn*, *pik3ca*, *actn1*, *erbb2*, *mapk14b*, *shc1*, *dido1* and *arvcfb* (Fig. 3B). In addition, we identified the hub genes of *psmd11b*, *psma3*, *ubqln4*, *hspa5*, *hspa9*, *hsp90aa1.2*, *usp14*, *psmd4a*, *psmc3* and *psmd14* in cluster 4 (Fig. 3C). In cluster 5, several DEGs were identified as hub genes, including *sgk1*, *skp2*, *fos*, *actb2*, *stat3*, *mapk8b*, *trrap*, *mcm2*, *cdk2* and *atr* (Fig. 3D). As well as in cluster 6, *ptk2*, *bptf*, *hdac4*, *actc1a*, *vcla*, *hsp90aa1.1*, *yes1*, *pik3ca*, *kat2b* and *ncor1* were identified as hub genes (Fig. 3E). For these hub genes, *pik3ca* was shared between cluster 3 and 6, and overlapped hub gene was found between clusters 4 and 5.

3.6. Pathway enrichment analysis of cluster genes

The pathway enrichment analysis results for the four clusters are shown in Fig. 4. In two significantly ($p < 0.05$) up-regulated clusters (cluster 4 and 5), the overlapping enriched pathways were glutathione metabolism, apoptosis, adipocytokine signaling pathway and phagosomes (Fig. 4B and Fig. 4C). Apart from these, DEGs in cluster 4 and 5 were significantly ($p < 0.05$) enriched in arachidonic acid metabolism, glycerolipid metabolism, insulin signaling pathway, FoxO signaling pathway, PPAR signaling pathway, MAPK signaling pathway, cell cycle, ubiquitin mediated proteolysis, proteasome and cell adhesion molecules. Moreover, in two significantly ($p < 0.05$) down-regulated clusters (cluster 3 and 6), the overlapping enriched pathways were ECM-receptor interaction, regulation of actin cytoskeleton and focal adhesion (Fig. 4A and Fig. 4D). Besides these, several significantly ($p < 0.05$) enriched pathways also comprised purine metabolism, starch and sucrose metabolism, adrenergic signaling in cardiomyocytes, endocytosis, ErbB signaling pathway and vascular smooth muscle contraction.

3.7. Alternative splicing events and associated pathways

As the results revealed, 571 DAS events were identified in the muscle tissues of spotted sea bass under low-temperature stress, including exon skipping (ES) and mutually exclusive exons (ME) types (Fig. 5A). Among them, 80.39 % ES and 19.61 % ME events accounted for the total number of DAS events, respectively. A gradually increasing trend was observed in the number of DAS events with prolongation of the low temperature. Additionally, 103 genes were overlapped between DEGs and DAS genes (Fig. 5B). Pathway enrichment of these overlapped genes showed that the glutathione metabolism, glycolysis / gluconeogenesis, focal adhesion, cysteine and methionine metabolism, ferroptosis, regulation of actin cytoskeleton, adipocytokine signaling pathway, adherens junction, FoxO signaling pathway, ErbB signaling pathway and insulin signaling pathway were significantly ($p < 0.05$) enriched (Fig. 5C).

From the pathway enrichment results of DEGs and DAS genes, ubiquitin mediated proteolysis and adipocytokine signaling pathway attracted our attention for their significant ($p < 0.05$) enrichment in the findings (Fig. 4 and Fig. 5C), indicating its significant ($p < 0.05$) role in responding to cold stress in spotted sea bass. Combining the published literatures and the results of this study, we summarized a presumptive schematic diagram that illustrates the response of the spotted sea bass to low-temperature stress (Fig. 6), and will be discussed in the Discussion section.

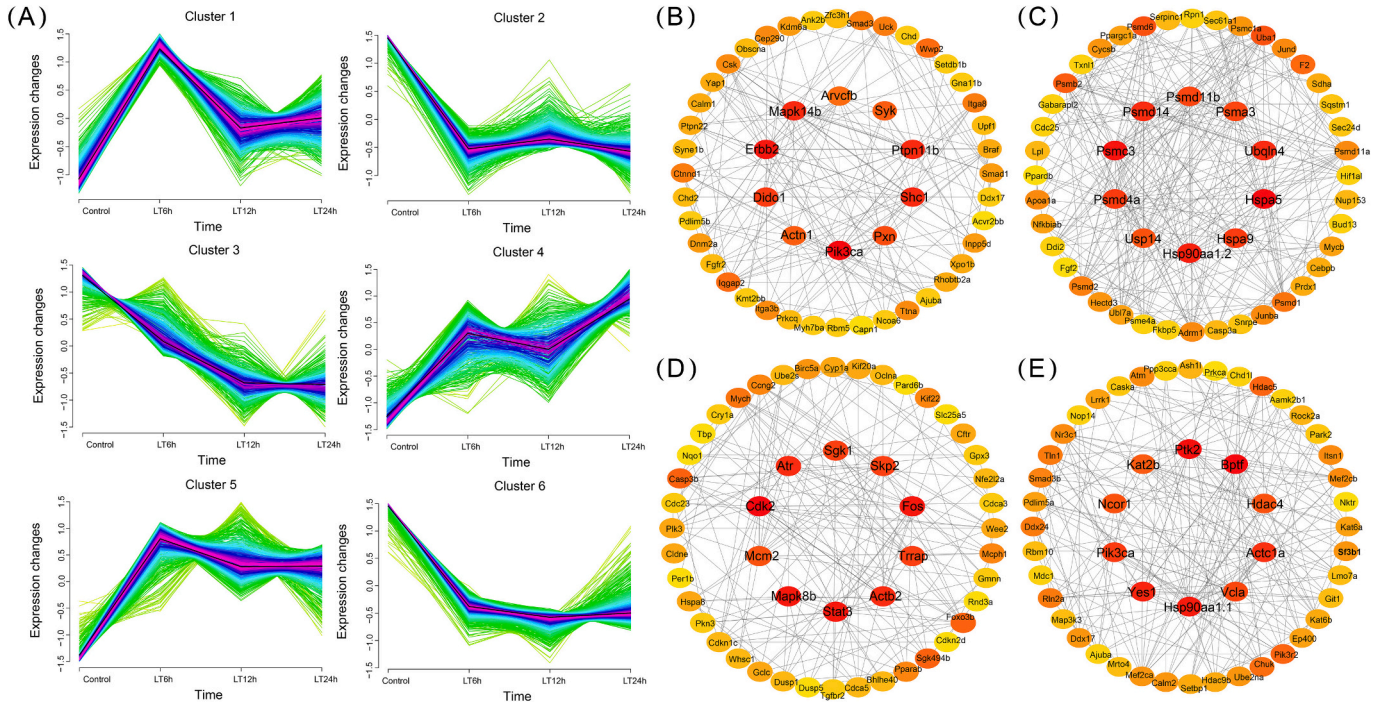

Fig. 3. (A) Results of the temporal expression analysis were classified into six clusters. Identification of hub genes in clusters 3 (B), clusters 4 (C), clusters 5 (D) and clusters 6 (E).

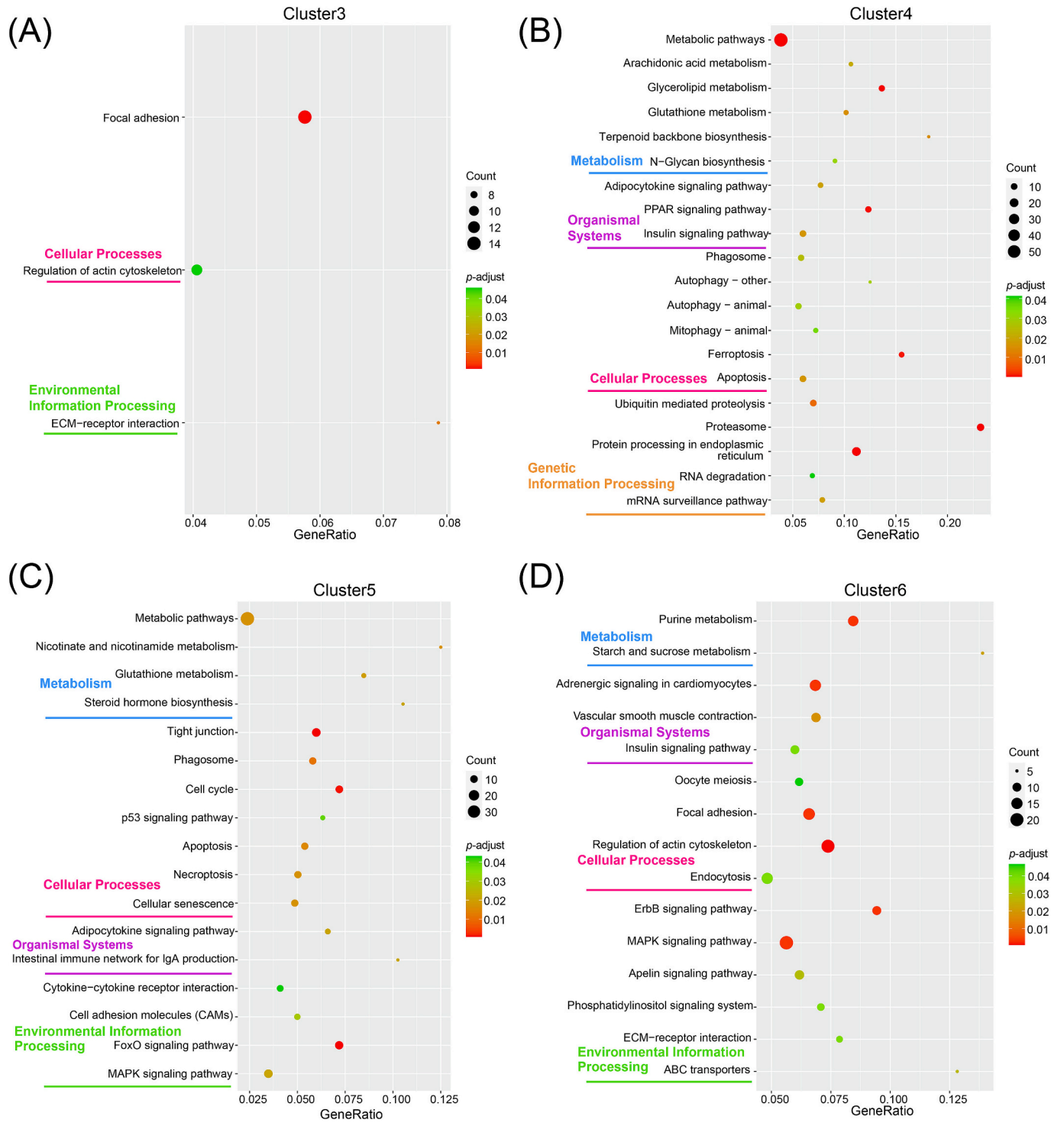

Fig. 4. Results of KEGG enrichment analysis in clusters 3 (A), clusters 4 (B), clusters 5 (C) and clusters 6 (D).

3.8. Validation of the transcriptome analysis

In this study, the relative expression levels of nine DEGs were validated by qPCR, with five up-regulated and four down-regulated DEGs, including *hspa5*, *psmc3*, *txnl1*, *stat3*, *fkbp5*, *myod1*, *ncor1*, *pnisr* and *pnn*. The results of the correlation analysis exhibited that a high correlation was present between the results of transcriptome analysis and the relative expression levels of these nine genes, with a correlation coefficient of 0.95 (Fig. 7), indicating the reliability of the results.

4. Discussion

As a poikilothermal species, temperature is the dominant environmental factor affecting the growth (Zhang et al., 2022), physiological metabolism (Cheng et al., 2017), mortality rate (Yilmaz et al., 2021) and behavior (Liu et al., 2024) in fish. When ambient temperatures are outside the tolerance range of fish, it can result in varying degrees of stress and even death. As an economically farmed fish, spotted sea bass has emerged as a dominant fish species for aquaculture in China (Zhang et al., 2023a, 2023b). However, the weak tolerance to low-temperature

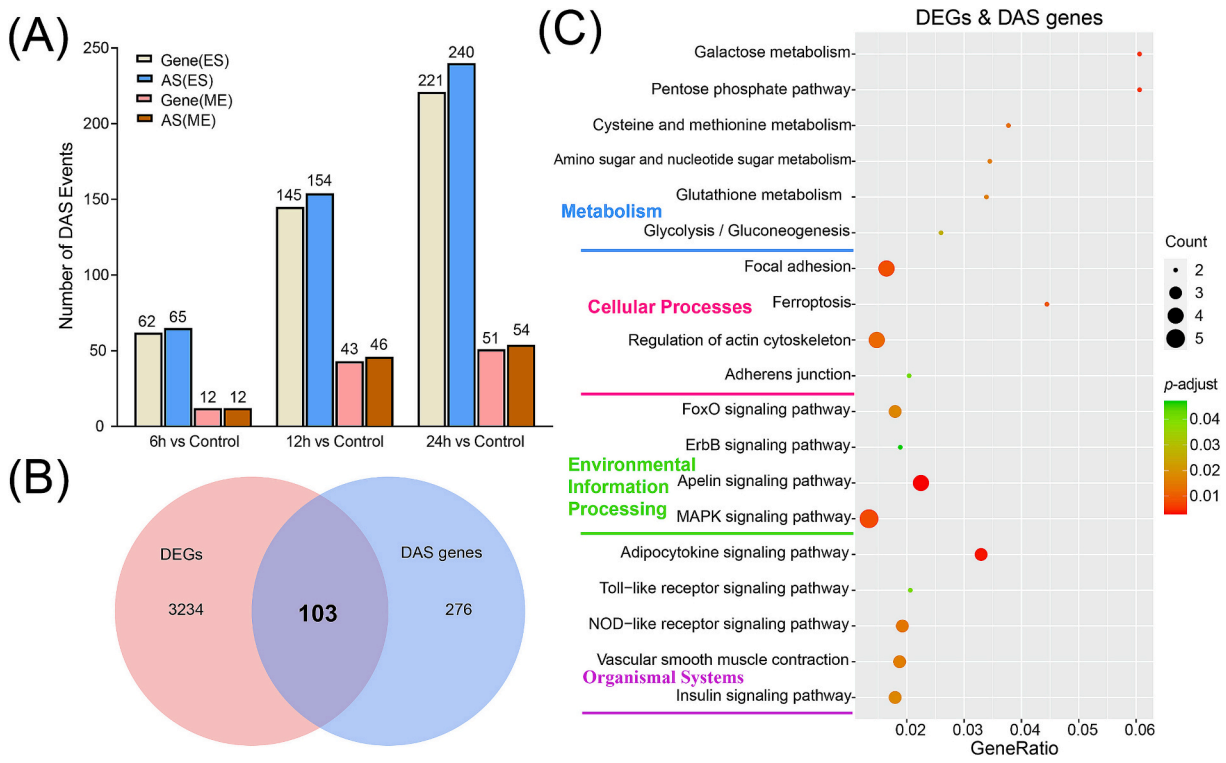

Fig. 5. (A) Identification of differential alternative splicing (DAS) events and genes. (B) Venn diagram of DAS genes and DEGs. (C) Results of KEGG enrichment analysis of overlapped genes between DAS genes and DEGs.

in the north winter makes it difficult to cope with the cold weather, which is susceptible to massive mortality, limiting sustainable aquaculture development. In this study, we measured dynamics in proximate composition and fatty acid profile after cold stress, and explored the transcriptional mechanisms of response to cold stress in spotted sea bass muscle tissue.

Crude protein and crude fat, essential for fish physiology, significantly ($p < 0.05$) decreased in spotted sea bass muscle under low-temperature stress, indicating their consumption during the stress response. Numerous studies have demonstrated that proteins and fats are used as predominant energy-storage molecule for low-temperature stress exposure (He et al., 2015). For instance, fat metabolism is regulated through the MAPK signaling pathway in *Takifugu fasciatus* to reduce muscle damage (Chu et al., 2021), while in tilapia (Chen et al., 2002) and larval zebrafish (Long et al., 2013), fat degradation and protein catabolism are activated to generate energy under cold stress. Additionally, moisture content in fish muscle is significantly ($p < 0.05$) influenced by temperature, with studies showing both increases and decreases in moisture levels during cold stress in species such as sturgeons (*Acipenser schrenckii*) (Zhang et al., 2023a, 2023b) and hybrid red tilapia (Refaey et al., 2023). The increase in moisture content may be explained by the fact that water is a carrier for biochemical reactions, which are heightened in response to low-temperature stress (Ball, 2008). Overall, muscle crude protein and crude fat contents in spotted sea bass significantly ($p < 0.05$) decreased, while moisture content increased to protect against low-temperature stress.

Previous reports discovered that the fatty acid profile of fish is strongly influenced by temperature (Khalili Tilami and Sampels, 2018). In this study, SFAs showed a significant decline ($p < 0.05$), while unsaturated fatty acids (UFAs) increased significantly ($p < 0.05$). Numerous studies have reported that lower water temperatures result in reduced content of SFAs and elevated content of UFAs. For example, increased levels of PUFA were found in juvenile genetically improved farmed tilapia (GIFT, *O. niloticus* L.) muscle after 72 h of short-term cold temperature experiment (He et al., 2015). Similar findings have been documented in various fish, including Atlantic salmon (*Salmo salar*) (Liu et al., 2020a, 2020b; Norambuena et al., 2016), carp (Trueman et al., 2000) and milkfish (*Chanos chanos*) (Hsieh and Kuo, 2005). Fatty acids are a major component of cell membranes, and their types can influence membrane function (Tocher, 2010). When subjected to low temperatures, fish prefer to increase the production of UFAs (PUFA and MUFA), and reduce SFAs to maintain the fluidity of cell membranes (Refaey et al., 2022). This adaptation contributes maintain normal membrane function and homeostasis under low temperature stress (Corrêa et al., 2018; Kostetsky et al., 2013). The gradual increase in the PUFA/SFA ratio further indicates that the content of SFA decreased, while PUFA was significantly increased ($p < 0.05$) during low-temperature stress. The dynamic changes between PUFA and SFA facilitate spotted sea bass to adapt to low-temperature stress.

For the DEGs in cluster 4, numerous ubiquitination-associated genes were found in the PPI network, including *psma3*, *psma4*, *psmb2*, *psmc1*, *psmc3*, *psmc4*, *psmc6*, *psmd1*, *psmd2*, *psmd4*, *psmd6*, *psmd7*, *psmd8*, *psmd11*, *psmd12*, *psmd14*, *psme3* and *psme4*. Moreover, ubiquitin mediated proteolysis pathway was significantly enriched ($p < 0.05$) for DEGs in cluster 4, implying that ubiquitin mediated protein degradation is essential for spotted sea bass to cope with low-temperature stress. Ubiquitination is the process by which proteins are targeted for degradation through the binding of ubiquitin proteins to substrate proteins (Ciechanover, 2005). Consequently, the ubiquitin mediated proteolysis pathway was activated, indicating enhanced degradation of unfolded or misfolded proteins induced by low temperatures. Previous findings showed that this pathway is significantly up-regulated ($p < 0.05$) in cold-tolerant fugu (*T. obscurus*) brain tissue (Han et al., 2022). Similarly, transcriptome analysis of brain and liver tissues from three Antarctic fish species revealed that protein degradation pathways associated with cold acclimation were also mediated by ubiquitination (Shin et al., 2012). Temperature compensation of the ubiquitin-proteasome pathway was found to adaptation to the cold in notothenioid fish (Todgham et al., 2017). Similar findings have been reported in other fish, including *Harpadon nehereus* (Sun et al., 2022), gilthead sea bream (*Sparus aurata*)

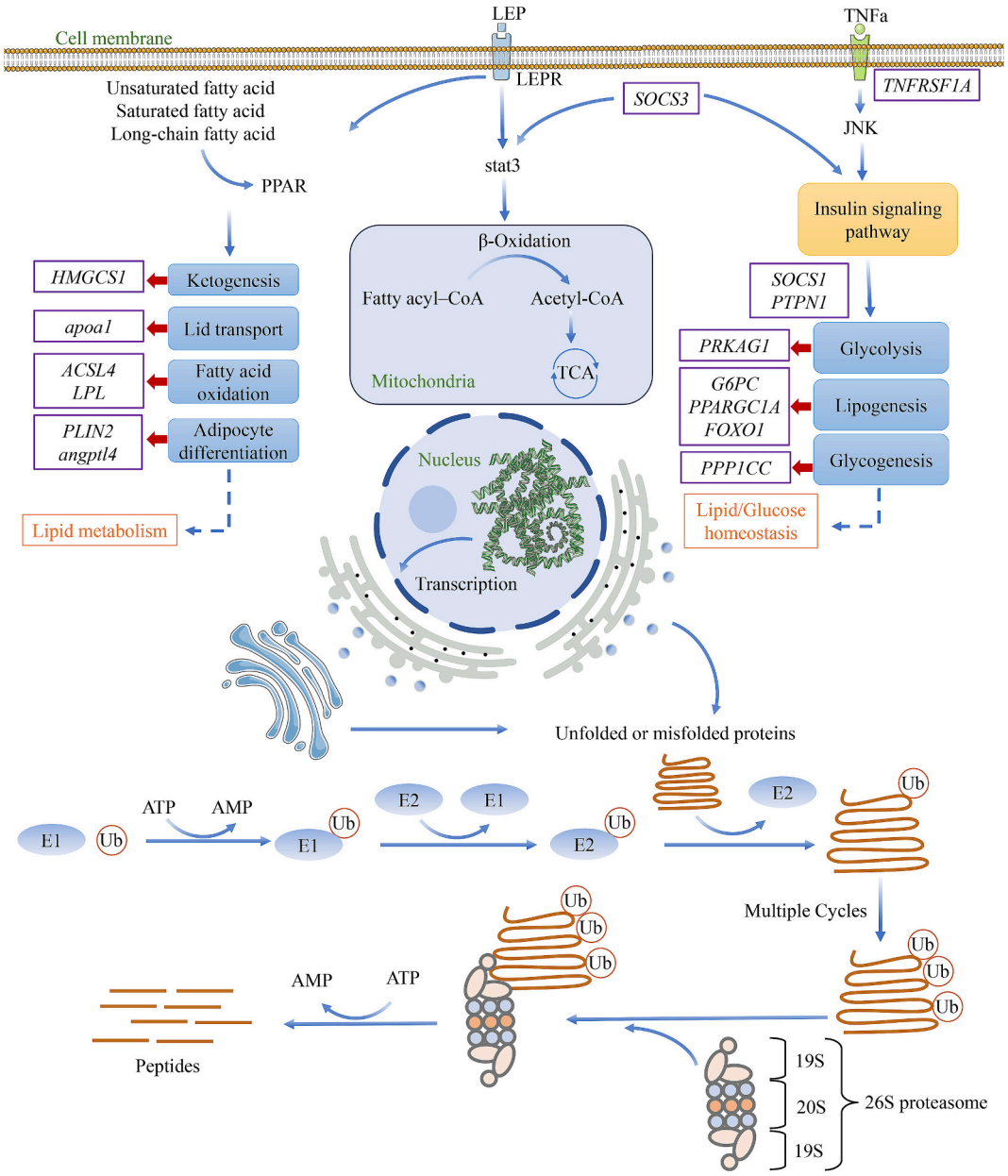

Fig. 6. Schematic diagram of the putative regulatory mechanism of the spotted sea bass muscle tissue in response to cold stress.

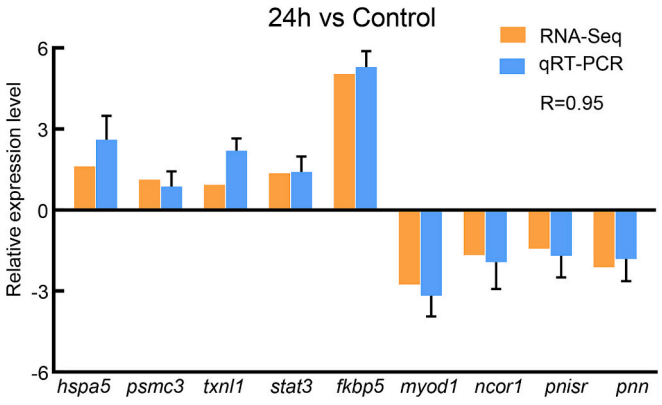

Fig. 7. Validation of RNA-seq results by qPCR.

(Ibarz et al., 2010), zebrafish (Long et al., 2013) and *Gymnocypris eckloni* (Nie et al., 2022). Consistent with previous studies, ubiquitin mediated proteolysis is a conserved molecular mechanism in spotted sea bass response to cold stress that removes unfolded or misfolded proteins and contributes to repair damaged cells in cold environments.

AS are a ubiquitous post-regulatory mechanism for gene expression that can significantly increase ($p < 0.05$) transcriptional diversity in eukaryotes (Punzo et al., 2020). Accumulating evidence suggests that AS plays a role as a regulator for adaptation under low-temperature stress. In zebrafish, 197 genes and 64 promoters were detected with AS events under low-temperature stress (Long et al., 2013). Comparative analyses of the levels of AS genes in three teleosts, including threespine stickleback (*Gasterosteus aculeatus*), Atlantic killifish and zebrafish, suggest that the AS respond to low-temperature is a frequent mechanism (Healy and Schulte, 2019). Spliceosomes, executors of AS events, were significantly up-regulated ($p < 0.05$) at low temperatures in medaka (*Oryzias latipes*) (Ikeda et al., 2017) and grass carp (*Ctenopharyngodon idellus*) (Shi et al., 2020). Similarly in spotted sea bass, 571 DAS events related to

low-temperatures stress were also identified, illustrating the key role of AS mechanism for cold acclimatization. As a member of the signal transducer and activator of transcription (STAT) proteins, the *stat3* gene was observed in both DEGs ang DAS genes, which regulates cell proliferation, differentiation, immune-related responses, and even environmental factor stress in fish (Bathige et al., 2017; Chen et al., 2023a, 2023b; Wang et al., 2019). For example, over-expression of the *lepa* gene reduced apoptosis through activation of STAT3, which acts as a protector under low temperature stress in a polar fish (*Dissostichus mawsoni*) (Wang et al., 2021). AS event of *stat3* will generate multiple transcript variant with multiplicity of effects in response to cold stress in spotted sea bass. Strong evidence suggested that *stat3* was also identified as a hub gene in the up-regulated expression of cluster 5 highlights the important role of this gene.

Furthermore, the *stat3* gene was observed in the adipocytokine signaling pathway that was enriched in both up-regulated cluster 4, and 5, as well as DAS genes. Adipocytokines are usually secreted by adipose tissue, comprising adiponectin, leptin and TNF-alpha (Tumor necrosis factor) being the most abundant adipocytokines (Tilg and Moschen, 2006). In this study, leptin and TNF-alpha were found in pathway enriched results. Leptin is an important regulator of energy intake and metabolic rate by regulating fatty acid β-oxidation and increasing energy expenditure through STAT3 phosphorylation. TNF-alpha, a pro-inflammatory adipocytokine, is linked to the insulin signaling pathway and is involved in regulating of insulin resistance. Several genes, including *G6PC*, *ACSL4*, *PLIN2* and *PPP1CC*, are associated with downstream functional responses that enhance lipid metabolism and maintain lipid / glucose homeostasis. Interestingly, long-chain fatty acid, UFAs and SFAs were regulated by adipocytokine signaling pathway, which could explain the significant ($p < 0.05$) changes in fatty acid composition and crude fat of spotted sea bass muscle tissues under low-temperature stress. The adipocytokine signaling pathway has been widely reported to be involved in cold stress response in fish. In Amur sleeper (*Perccottus glenii*), the highest levels of DEGs associated with the adipocytokine signaling pathway were found by comparing control and freezing treatment groups (Ning et al., 2024). Transcriptomic sequencing in *Schizothorax wangchiachii* muscles tissue revealed that DEGs were mainly enriched in the adipocytokine signaling pathway under low-temperature stress (Zhao et al., 2024). Similar results have been found in other fish, including red-tail catfish (*Hemibagrus wyckioides*) (Liu et al., 2022a, 2022b), largemouth bass (*Micropterus salmoides*) (Yu et al., 2023), pearl gentian grouper (*Epinephelus fuscoguttatus* ♀ × *E. lanceolatus* ♂) (Miao et al., 2021) and tiger puffer (*T. rubripes*) (Liu et al., 2022a, 2022b). These evidences implicate that the regulation of lipid metabolism through adipocyte signaling pathways is an essential molecular mechanism in response to low-temperature stress in fish.

5. Conclusion

In summary, we investigated the dynamics of proximate composition and fatty acid profile, and elucidated the molecular mechanisms underlying the response to low-temperature stress in spotted sea bass muscle tissue through transcriptomic analysis. Significant ($p < 0.05$) changes in crude fat, crude protein and moisture content were observed for proximate composition. Furthermore, the decrease in saturated fatty acids (SFAs) and increase in unsaturated fatty acids (UFAs) were found in fatty acid profile. Bioinformatics analysis of the transcriptomic data identified 3337 differentially expressed genes (DEGs), which were clustered into six groups, and differential alternative splicing (DAS) events were also detected. KEGG pathway enrichment analysis of these genes highlighted the roles of ubiquitin-mediated protein proteolysis and adipocytokine signaling pathways in explaining the observed changes in the proximate composition and fatty acid profile. Overall, these findings contribute to the understanding of the impact of low-temperature stress on spotted sea bass and offer novel insights for improving culture management in future and studying cold stress mechanisms in fish.

However, this study has certain limitations. The long-term effects of low-temperature stress on the physiological and molecular adaptations of spotted sea bass were not explored, and potential interactions between muscle tissue and other tissues, such as the liver and gills, remain unaddressed. These gaps highlight opportunities for future research to build on the current findings and deepen our understanding of fish responses to low-temperature stress.

Funding

This work was supported by National Natural Science Foundation of China -Joint Fund Key Program Project [grant number: U24A20456], National Key Research and Development Program of China [grant number: 2022YFD2400103] and China Agriculture Research System (CARS for Marine Fish Culture Industry) [grant number: CARS-47].

CRediT authorship contribution statement

Cong Liu: Writing – original draft, Methodology, Conceptualization. **Yuan Zheng:** Software, Methodology. **Haishen Wen:** Methodology, Funding acquisition. **Chong Zhang:** Visualization, Methodology. **Yonghang Zhang:** Software, Methodology. **Lingyu Wang:** Visualization, Software. **Donglei Sun:** Software, Data curation. **Kaiqiang Zhang:** Visualization, Methodology. **Xin Qi:** Resources, Conceptualization. **Yun Xia:** Writing – review & editing, Software, Methodology. **Yun Li:** Writing – review & editing, Methodology, Funding acquisition.

Declaration of competing interest

The corresponding authors state that there are no conflicts of interest.

Appendix A. Supplementary data

Supplementary data to this article can be found online at https://doi.org/10.1016/j.aquaculture.2025.742139.

Data availability

Data will be made available on request.

References

Ahmed, I., Jan, K., Fatma, S., Dawood, M.A.O., 2022. Muscle proximate composition of various food fish species and their nutritional significance: a review. J. Anim. Physiol. Anim. Nutr. 106, 690–719. https://doi.org/10.1111/jpn.13711.

Araújo, B.C., Rodriguez, M., Honji, R.M., Rombenso, A.N., del Rio-Zaragoza, O.B., Cano, A., Tinajero, A., Mata-Sotres, J.A., Viana, M.T., 2021. Arachidonic acid modulated lipid metabolism and improved productive performance of striped bass (*Morone saxatilis*) juvenile under sub- to optimal temperatures. Aquaculture 530, 735939. https://doi.org/10.1016/j.aquaculture.2020.735939.

Bai, Y., Ding, X., Liu, Z., Shen, J., Huang, Y., 2022. Identification and functional analysis of circRNAs in the skeletal muscle of juvenile and adult largemouth bass (*Micropterus salmoides*). Comp. Biochem. Physiol. Part D Genom. Proteom. 42, 100969. https://doi.org/10.1016/j.cbd.2022.100969.

Ball, P., 2008. Water as an active constituent in cell biology. Chem. Rev. 108, 74–108. https://doi.org/10.1021/cr068037a.

Bathige, S.D.N.K., Thulasitha, W.S., Umasuthan, N., Jayasinghe, J.D.H.E., Wan, Q., Nam, B.-H., Lee, J., 2017. A homolog of teleostean signal transducer and activator of transcription 3 (STAT3) from rock bream, *Oplegnathus fasciatus*: structural insights, transcriptional modulation, and subcellular localization. Vet. Immunol. Immunopathol. 186, 29–40. https://doi.org/10.1016/j.vetimm.2017.02.008.

Biederman, A.M., O'Brien, K.M., Crockett, E.L., 2021. Homeoviscous adaptation occurs with thermal acclimation in biological membranes from heart and gill, but not the brain, in the Antarctic fish *Notothenia coriiceps*. J. Comp. Physiol. B. 191, 289–300. https://doi.org/10.1007/s00360-020-01339-5.

Bolger, A.M., Lohse, M., Usadel, B., 2014. Trimmomatic: a flexible trimmer for Illumina sequence data. Bioinformatics 30, 2114–2120. https://doi.org/10.1093/bioinformatics/btu170.

Bu, D., Luo, H., Huo, P., Wang, Z., Zhang, S., He, Z., Wu, Y., Zhao, L., Liu, J., Guo, J., Fang, S., Cao, W., Yi, L., Zhao, Y., Kong, L., 2021. KOBAS-i: intelligent prioritization

and exploratory visualization of biological functions for gene enrichment analysis. Nucleic Acids Res. 49, W317–W325. https://doi.org/10.1093/nar/gkab447.
Chen, W.-H., Sun, L.-T., Tsai, C.-L., Song, Y.-L., Chang, C.-F., 2002. Cold-stress induced the modulation of Catecholamines, cortisol, immunoglobulin M, and leukocyte phagocytosis in Tilapia. Gen. Comp. Endocrinol. 126, 90–100. https://doi.org/10.1006/gcen.2001.7772.
Chen, J., Han, P., Liu, X., Wang, X., 2023a. Characterization of Japanese flounder (*Paralichthys olivaceus*) STAT members: an immune-related gene family involved in Edwardsiella tarda and temperature stress. Fish Shellfish Immunol. 138, 108818. https://doi.org/10.1016/j.fsi.2023.108818.
Chen, B., Zhou, Z., Shi, Y., Gong, J., Li, C., Zhou, T., Li, Y., Zhang, D., Xu, P., 2023b. Genome-wide evolutionary signatures of climate adaptation in spotted sea bass inhabiting different latitudinal regions. Evol. Appl. 16, 1029–1043. https://doi.org/10.1111/eva.13551.
Cheng, C.-H., Ye, C.-X., Guo, Z.-X., Wang, A.-L., 2017. Immune and physiological responses of pufferfish (*Takifugu obscurus*) under cold stress. Fish Shellfish Immunol. 64, 137–145. https://doi.org/10.1016/j.fsi.2017.03.003.
Chu, P., Wang, T., Sun, Y.R., Chu, M.X., Wang, H.Y., Zheng, X., Yin, S., 2021. Effect of cold stress on the MAPK pathway and lipidomics on muscle of *Takifugu fasciatus*. Aquaculture 540, 736691. https://doi.org/10.1016/j.aquaculture.2021.736691.
Ciechanover, A., 2005. Proteolysis: from the lysosome to ubiquitin and the proteasome. Nat. Rev. Mol. Cell Biol. 6, 79–87. https://doi.org/10.1038/nrm1552.
Corrêa, C.F., Nobrega, R.O., Block, J.M., Fracalossi, D.M., 2018. Mixes of plant oils as fish oil substitutes for *Nile tilapia* at optimal and cold suboptimal temperature. Aquaculture 497, 82–90. https://doi.org/10.1016/j.aquaculture.2018.07.034.
Deng, W., Sun, J., Chang, Z.-G., Gou, N.-N., Wu, W.-Y., Luo, X.-L., Zhou, J.-S., Yu, H.-B., Ji, H., 2020. Energy response and fatty acid metabolism in *Onychostoma macrolepis* exposed to low-temperature stress. J. Therm. Biol. 94, 102725. https://doi.org/10.1016/j.jtherbio.2020.102725.
Dietrich, M.A., Hliwa, P., Adamek, M., Steinhagen, D., Karol, H., Ciereszko, A., 2018. Acclimation to cold and warm temperatures is associated with differential expression of male carp blood proteins involved in acute phase and stress responses, and lipid metabolism. Fish Shellfish Immunol. 76, 305–315. https://doi.org/10.1016/j.fsi.2018.03.018.
Gong, J., Chen, B., Li, B., Zhou, Z., Shi, Y., Ke, Q., Zhang, D., Xu, P., 2020. Genetic analysis of whole mitochondrial genome of *Lateolabrax maculatus* (Perciformes: Moronidae) indicates the presence of two populations along the Chinese coast. Zoologia 37, 1–12. https://doi.org/10.3109/19401736.2015.1115496.
Han, S., Wei, S., Chen, R., Ni, M., Chen, L., 2022. Tissue-specific and differential cold responses in the domesticated cold tolerant Fugu. Fishes 7 (4). https://doi.org/10.3390/fishes7040159.
He, J., Qiang, J., Yang, H., Xu, P., Zhu, Z.X., Yang, R.Q., 2015. Changes in the fatty acid composition and regulation of antioxidant enzymes and physiology of juvenile genetically improved farmed tilapia *Oreochromis niloticus* (L.), subjected to short-term low temperature stress. J. Therm. Biol. 53, 90–97. https://doi.org/10.1016/j.jtherbio.2015.08.010.
Healy, T.M., Schulte, P.M., 2019. Patterns of alternative splicing in response to cold acclimation in fish. J. Exp. Biol. 222, jeb193516. https://doi.org/10.1242/jeb.193516.
Hsieh, S.L., Kuo, C.M., 2005. Stearoyl–CoA desaturase expression and fatty acid composition in milkfish (*Chanos chanos*) and grass carp (*Ctenopharyngodon idella*) during cold acclimation. Comp. Biochem. Physiol. B. Biochem. Mol. Biol. 141, 95–101. https://doi.org/10.1016/j.cbpc.2005.02.001.
Ibarz, A., Blasco, J., Beltrán, M., Gallardo, M.A., Sánchez, J., Sala, R., Fernández-Borràs, J., 2005. Cold-induced alterations on proximate composition and fatty acid profiles of several tissues in gilthead sea bream (*Sparus aurata*). Aquaculture 249, 477–486. https://doi.org/10.1016/j.aquaculture.2005.02.056.
Ibarz, A., Martín-Pérez, M., Blasco, J., Bellido, D., de Oliveira, E., Fernández-Borràs, J., 2010. Gilthead Sea bream liver proteome altered at low temperatures by oxidative stress. Proteomics 10, 963–975. https://doi.org/10.1002/pmic.200900528.
Ikeda, D., Koyama, H., Mizusawa, N., Kan-no, N., Tan, E., Asakawa, S., Watabe, S., 2017. Global gene expression analysis of the muscle tissues of medaka acclimated to low and high environmental temperatures. Comp. Biochem. Physiol. Part D Genom. Proteom. 24, 19–28. https://doi.org/10.1016/j.cbd.2017.07.002.
Khalili Tilami, S., Sampels, S., 2018. Nutritional value of fish: lipids, proteins, vitamins, and minerals. Rev. Fish Sci. Aquac. 26, 243–253. https://doi.org/10.1080/23308249.2017.1399104.
Kim, D., Paggi, J.M., Park, C., Bennett, C., Salzberg, S.L., 2019. Graph-based genome alignment and genotyping with HISAT2 and HISAT-genotype. Nat. Biotechnol. 37, 907–915. https://doi.org/10.1038/s41587-019-0201-4.
Kostetsky, E.Y., Velansky, P.V., Sanina, N.M., 2013. Phase transitions of phospholipids as a criterion for assessing the capacity for thermal adaptation in fish. Russ. J. Mar. Biol. 39, 214–222. https://doi.org/10.1134/S1063074013030073.
Kumar, L., Futschik, M.E., 2007. Mfuzz: a software package for soft clustering of microarray data. Bioinformation 2, 5–7. https://doi.org/10.6026/97320630002005.
Liao, Y., Smyth, G.K., Shi, W., 2014. featureCounts: an efficient general purpose program for assigning sequence reads to genomic features. Bioinformatics 30, 923–930. https://doi.org/10.1093/bioinformatics/btt656.
Liu, F., Chu, T., Wang, M., Zhan, W., Xie, Q., Lou, B., 2020a. Transcriptome analyses provide the first insight into the molecular basis of cold tolerance in *Larimichthys polyactis*. J. Comp. Physiol. B. 190, 27–34. https://doi.org/10.1007/s00360-019-01247-3.
Liu, C., Ge, J., Zhou, Y., Thirumurugan, R., Gao, Q., Dong, S., 2020b. Effects of decreasing temperature on phospholipid fatty acid composition of different tissues and hematology in Atlantic salmon (*Salmo salar*). Aquaculture 515, 734587. https://doi.org/10.1016/j.aquaculture.2019.734587.
Liu, M., Zhou, Y.-L., Guo, X.-F., Wei, W.-Y., Li, Z., Zhou, L., Wang, Z.-W., Gui, J.-F., 2022a. Comparative transcriptomes and metabolomes reveal different tolerance mechanisms to cold stress in two different catfish species. Aquaculture 560, 738543. https://doi.org/10.1016/j.aquaculture.2022.738543.
Liu, Z., Zhu, L., Wang, X., Liu, S., Ma, A., Chang, H., Sun, Z., Xu, F., Zhao, H., 2022b. Application of transcriptome analysis to investigate the effects of long-term low temperature stress on liver function in the tiger puffer (*Takifugu rubripes*). Front. Mar. Sci. 9. https://doi.org/10.3389/fmars.2022.1069711.
Liu, C., Li, J., Qi, X., Wang, L., Sun, D., Zhang, J., Zhang, K., Li, J., Li, Y., Wen, H., 2023. Cytochrome P450 superfamily in spotted sea bass: genome-wide identification and expression profiles under trichlorfon and environmental stresses. Comp. Biochem. Physiol. Part D Genom. Proteom. 46, 101078. https://doi.org/10.1016/j.cbd.2023.101078.
Liu, S.-T., Chang, C.-Y., Lee, K.-Y., Tong, S.-K., Huang, H.-L., Chen, H., Horng, J.-L., Chou, M.-Y., 2024. Alternation of social behaviors for zebrafish (*Danio rerio*) in response to acute cold stress. Fish Physiol. Biochem. 50, 653–666. https://doi.org/10.1007/s10695-024-01296-8.
Long, Y., Song, G., Yan, J., He, X., Li, Q., Cui, Z., 2013. Transcriptomic characterization of cold acclimation in larval zebrafish. BMC Genomics 14, 612. https://doi.org/10.1186/1471-2164-14-612.
Love, M.I., Huber, W., Anders, S., 2014. Moderated estimation of fold change and dispersion for RNA-seq data with DESeq2. Genome Biol. 15, 550. https://doi.org/10.1186/s13059-014-0550-8.
Miao, B.-B., Niu, S.-F., Wu, R.-X., Liang, Z.-B., Tang, B.-G., Zhai, Y., Xu, X.-Q., 2021. Gene expression profile and co-expression network of pearl gentian grouper under cold stress by integrating Illumina and PacBio sequences. Animals 11 (6). https://doi.org/10.3390/ani11061745.
Nie, M., Ni, W., Wang, L., Gao, Q., Liu, D., Tian, F., Wang, Z., Zhang, C., Qi, D., 2022. Insights into miRNA-mRNA regulatory mechanisms of cold adaptation in *Gymnocypris eckloni*: ubiquitin-mediated proteolysis is pivotal for adaptive energy metabolism. Front. Genet. 13. https://doi.org/10.3389/fgene.2022.903995.
Ning, Z., Chen, Y., Wang, Z., Zhou, H., Sun, M., Yao, T., Mu, W., 2024. Transcriptome, histological, and physiological responses of Amur sleeper (*Perccottus glenii*) during cold stress, freezing, and recovery. Comp. Biochem. Physiol. Part D Genom. Proteom. 49, 101192. https://doi.org/10.1016/j.cbd.2024.101192.
Norambuena, F., Rombenso, A., Turchini, G.M., 2016. Towards the optimization of performance of Atlantic salmon reared at different water temperatures via the manipulation of dietary ARA/EPA ratio. Aquaculture 450, 48–57. https://doi.org/10.1016/j.aquaculture.2015.06.044.
Polley, S.D., Tiku, P.E., Trueman, R.T., Caddick, M.X., Morozov, I.Y., Cossins, A.R., 2003. Differential expression of cold- and diet-specific genes encoding two carp liver Δ9-acyl-CoA desaturase isoforms. Am. J. Phys. Regul. Integr. Comp. Phys. 284, R41–R50. https://doi.org/10.1152/ajpregu.00263.2002.
Punzo, P., Grillo, S., Batelli, G., 2020. Alternative splicing in plant abiotic stress responses. Biochem. Soc. Trans. 48, 2117–2126. https://doi.org/10.1042/bst20200281.
Refaey, M.M., Mehrim, A.I., Zenhom, O.A., Mansour, A.T., 2022. Effect of fatty acids manipulation on survival and physiological response of hybrid red tilapia under chronic cold stress. Aquaculture 561, 738663. https://doi.org/10.1016/j.aquaculture.2022.738663.
Refaey, M.M., Mehrim, A.I., El-Komy, M.M., Zenhom, O.A., Mansour, A.T., 2023. Chronic cold-stress induced histopathological changes, oxidative stress, and alterations in liver functions and nutrient composition of hybrid red tilapia and the potential protection of unsaturated fatty acids. Front. Mar. Sci. 10. https://doi.org/10.3389/fmars.2023.1148978.
Ren, Y., Tian, Y., Mao, X., Wen, H., Qi, X., Li, J., Li, J., Li, Y., 2022. Acute hypoxia changes the gene expression profiles and alternative splicing landscape in gills of spotted sea bass (*Lateolabrax maculatus*). Front. Mar. Sci. 9. https://doi.org/10.3389/fmars.2022.1024218.
Shaklee, J.B., Christiansen, J.A., Sidell, B.D., Prosser, C.L., Whitt, G.S., 1977. Molecular aspects of temperature acclimation in fish: contributions of changes in enzyme activities and isozyme patterns to metabolic reorganization in the green sunfish. J. Exp. Zool. 201, 1–20. https://doi.org/10.1002/jez.1402010102.
Shannon, P., Markiel, A., Ozier, O., Baliga, N.S., Wang, J.T., Ramage, D., Amin, N., Schwikowski, B., Ideker, T., 2003. Cytoscape: a software environment for integrated models of biomolecular interaction networks. Genome Res. 13, 2498–2504. https://doi.org/10.1101/gr.1239303.
Shen, S., Park, J.W., Lu, Z.X., Lin, L., Henry, M.D., Wu, Y.N., Zhou, Q., Xing, Y., 2014. rMATS: robust and flexible detection of differential alternative splicing from replicate RNA-Seq data. PNAS 111, E5593–E5601. https://doi.org/10.1073/pnas.1419161111.
Shi, M., Zhang, Q., Li, Y., Zhang, W., Liao, L., Cheng, Y., Jiang, Y., Huang, X., Duan, Y., Xia, L., Ye, W., Wang, Y., Xia, X.-Q., 2020. Global gene expression profile under low-temperature conditions in the brain of the grass carp (*Ctenopharyngodon idellus*). PLoS One 15, e0239730. https://doi.org/10.1371/journal.pone.0239730.
Shin, S.C., Kim, S.J., Lee, J.K., Ahn, D.H., Kim, M.G., Lee, H., Lee, J., Kim, B.-K., Park, H., 2012. Transcriptomics and comparative analysis of three Antarctic Notothenioid fishes. PLoS One 7, e43762. https://doi.org/10.1371/journal.pone.0043762.
Sun, Z., Tan, X., Liu, Q., Ye, H., Zou, C., Xu, M., Zhang, Y., Ye, C., 2019. Physiological, immune responses and liver lipid metabolism of orange-spotted grouper (*Epinephelus coioides*) under cold stress. Aquaculture 498, 545–555. https://doi.org/10.1016/j.aquaculture.2018.08.051.
Sun, Z., Huang, L., Kong, Y., Wang, L., Kang, B., 2022. Regulating strategies of transcription and alternative splicing for cold tolerance *Harpadon nehereus* fish. Front. Ecol. Evol. 10. https://doi.org/10.3389/fevo.2022.912113.

Tilg, H., Moschen, A.R., 2006. Adipocytokines: mediators linking adipose tissue, inflammation and immunity. Nat. Rev. Immunol. 6, 772–783. https://doi.org/10.1038/nri1937.

Tocher, D.R., 2010. Fatty acid requirements in ontogeny of marine and freshwater fish. Aquac. Res. 41, 717–732. https://doi.org/10.1111/j.1365-2109.2008.02150.x.

Todgham, A.E., Crombie, T.A., Hofmann, G.E., 2017. The effect of temperature adaptation on the ubiquitin–proteasome pathway in notothenioid fishes. J. Exp. Biol. 220, 369–378. https://doi.org/10.1242/jeb.145946.

Trueman, R.J., Tiku, P.E., Caddick, M.X., Cossins, A.R., 2000. Thermal thresholds of lipid restructuring and delta(9)-desaturase expression in the liver of carp (*Cyprinus carpio* L.). J. Exp. Biol. 203, 641–650. https://doi.org/10.1242/jeb.203.3.641.

Wang, T., Lin, P., Guo, S., Wang, Y., Zhang, Z., Feng, J., 2019. Molecular characterization and expression analysis of signal transducer and activator of transcription 1 (STAT1) in Japanese eel *Anguilla japonica*. Fish Shellfish Immunol. 86, 956–964. https://doi.org/10.1016/j.fsi.2018.12.046.

Wang, Y., Wang, H., Hu, L., Chen, L., 2021. Leptin gene protects against cold stress in Antarctic toothfish. Front. Physiol. 12. https://doi.org/10.3389/fphys.2021.740806.

Wang, Z., Dong, Z., Yang, Y., Wang, J., Yang, T., Chen, X., Liang, L., Mu, W., 2022. Histology, physiology, and glucose and lipid metabolism of *Lateolabrax maculatus* under low temperature stress. J. Therm. Biol. 104, 103161. https://doi.org/10.1016/j.jtherbio.2021.103161.

Wang, Y., Chen, Z., Wei, M., Lin, Z., Shen, M., Zhu, F., Jia, C., Meng, Q., Xu, D., Du, S., Liu, Y., Chen, S., Zhang, C., Zhang, Z., Zhang, Z., 2023. Liver transcriptome analysis of the black porgy (*Acanthopagrus schlegelii*) under acute low-temperature stress. Life 13, 721. https://doi.org/10.3390/life13030721.

Wickham, H., 2011. ggplot2. WIREs Comp. Stat. 3, 180–185. https://doi.org/10.1002/wics.147.

Yilmaz, S., Ergün, S., Çelik, E.Ş., Banni, M., Ahmadifar, E., Dawood, M.A.O., 2021. The impact of acute cold water stress on blood parameters, mortality rate and stress-related genes in *Oreochromis niloticus*, *Oreochromis mossambicus* and their hybrids. J. Therm. Biol. 100, 103049. https://doi.org/10.1016/j.jtherbio.2021.103049.

Yu, J., Zhong, D., Li, S., Zhang, Z., Mo, H., Wang, L., 2023. Acute temperature stresses trigger liver transcriptome and microbial community remodeling in largemouth bass (*Micropterus salmoides*). Aquaculture 573, 739573. https://doi.org/10.1016/j.aquaculture.2023.739573.

Zhang, Z., Zhou, C., Fan, K., Zhang, L., Liu, Y., Liu, P.-F., 2021. Metabolomics analysis of the effects of temperature on the growth and development of juvenile European seabass (*Dicentrarchus labrax*). Sci. Total Environ. 769, 145155. https://doi.org/10.1016/j.scitotenv.2021.145155.

Zhang, M., Hu, J., Zhu, J., Wang, Y., Zhang, Y., Li, Y., Xu, S., Yan, X., Zhang, D., 2022. Transcriptome, antioxidant enzymes and histological analysis reveal molecular mechanisms responsive to long-term cold stress in silver pomfret (*Pampus argenteus*). Fish Shellfish Immunol. 121, 351–361. https://doi.org/10.1016/j.fsi.2022.01.017.

Zhang, C., Wen, H., Zhang, Y., Zhang, K., Qi, X., Li, Y., 2023a. First genome-wide association study and genomic prediction for growth traits in spotted sea bass (*Lateolabrax maculatus*) using whole-genome resequencing. Aquaculture 566, 739194. https://doi.org/10.1016/j.aquaculture.2022.739194.

Zhang, T., Zhang, L., Yin, T., You, J., Liu, R., Huang, Q., Shi, L., Wang, L., Liao, T., Wang, W., Ma, H., 2023b. Recent understanding of stress response on muscle quality of fish: from the perspective of industrial chain. Trends Food Sci. Technol. 140, 104145. https://doi.org/10.1016/j.tifs.2023.104145.

Zhao, Y.F., Peng, W.Z., Guo, H.Y., Chen, B.H., Zhou, Z.X., Xu, J., Zhang, D.C., Xu, P., 2018. Population genomics reveals genetic divergence and adaptive differentiation of Chinese Sea bass (*Lateolabrax maculatus*). Mar. Biotechnol. 20, 45–59. https://doi.org/10.1007/s10126-017-9786-0.

Zhao, H., Zhao, Z., Liu, C., Zhou, J., Huang, Z., Duan, Y., Zhang, L., Ke, H., Du, J., Mou, C., Li, Q., 2024. An integrated analysis of transcriptome and metabolome to reveal the effects of temperature stress on energy metabolism and physiological responses in *Schizothorax wangchiachii* muscles. Aquaculture 591, 741103. https://doi.org/10.1016/j.aquaculture.2024.741103.

Zuo, R., Ai, Q., Mai, K., Xu, W., Wang, J., Xu, H., Liufu, Z., Zhang, Y., 2012. Effects of dietary n-3 highly unsaturated fatty acids on growth, nonspecific immunity, expression of some immune related genes and disease resistance of large yellow croaker (*Larmichthys crocea*) following natural infestation of parasites (*Cryptocaryon irritans*). Fish Shellfish Immunol. 32, 249–258. https://doi.org/10.1016/j.fsi.2011.11.005.